Robotica (2016) volume 34, pp. 258–273. © Cambridge University Press 2014
doi:10.1017/S0263574714001416

Multi-objective optimal design based kineto-elastostatic performance for the DELTA parallel mechanism

Belkacem Bounab*

Laboratoire de Mécanique des Structures, École Militaire Polytechnique
BP 17, 16111-Bordj El-Bahri, Algiers, Algeria

(Accepted May 2, 2014. First published online: June 4, 2014)

SUMMARY

This paper addresses the dimensional-synthesis-based kineto-elastostatic performance optimization of the DELTA parallel mechanism. For the manipulator studied here, the main consideration for the optimization criteria is to find the maximum regular workspace where the robot DELTA must posses high stiffness and dexterity. The dexterity is a kinetostatic quality measure that is related to joint's stiffness and control accuracy. In this study, we use the Castigliano's energetic theorem for modeling the elastostatic behavior of the DELTA parallel robot, which can be evaluated by the mechanism's response to external applied wrench under static equilibrium. In the proposed formulation of the design problem, global structure's stiffness and global dexterity are considered together for the simultaneous optimization. Therefore, we formulate the design problem as a multi-objective optimization one and, we use evolutionary genetic algorithms to find all possible trade-offs among multiple cost functions that conflict with each other. The proposed design procedure is developed through the implementation of the DELTA robot and, numerical results show the effectiveness of the proposed design method to enhancing kineto-elastostatic performance of the studied manipulator's structure.

KEYWORDS: DELTA robot; Optimal design; Kineto-elastostatic performance; Multi-objective optimization; Evolutionary algorithms.

Nomenclature

$\mathbf{s}$	Center of the moving platform.
$\mathbf{q}$	Active joint variables.
$\dot{\mathbf{s}}$	Cartesian velocity of the moving platform.
$\dot{\mathbf{q}}$	Active joint velocities.
$\beta_i,\ \gamma_i$	Passive joint variables ($i = 1 \ldots 3$).
J	Kinematic Jacobian matrix.
C	Compliance matrix of the mechanism.
$\kappa_F,\ \mu$	Frobenius condition number and conditioning index of J.
$\mu_{\min},\ \mu^{\text{adm}}$	Global minimum and imposed (threshold) value of conditioning index.
$\delta_s,\ \theta_s$	Displacement and orientation of moving platform.
$r_{ball},\ z_0$	Radius and center of the maximum inscribed spherical workspace.
$l_p,\ l_d$	Lengths of proximal and distal links.
$l_{\max}$	Maximum imposed length of a subchain.
$\mathbf{N}_d \in \mathbb{R}^6$	Internal axial forces in distal links.
$\mathbf{w}_{ext} \in \mathbb{R}^6$	External applied wrench w.r.t. $\mathbf{s}$.

* Corresponding author. E-mail: bounabbelkacem.emp@gmail.com

https://doi.org/10.1017/S0263574714001416 Published online by Cambridge University Press

$\mathbf{F}_p^i \in \mathbb{R}^6$	Internal forces and moments in proximal links ($i = 1 \ldots 3$).
$E_d,\ E_p$	Elasticity modulus of distal and proximal links.
G_p	Shear modulus of proximal links.
$k_y,\ k_z$	Shear correction constants.
$I_{yp},\ I_{zp},\ J_p$	Bending and polar moments of inertia of proximal.
$A_d,\ A_p$	Cross-sectional areas of distal and proximal links.
m_0	Mass of proximal and distal bodies.
$b \times h$	Dimensions of the proximal rectangular cross-section.
ϕ_d	Diameter of the distal circular cross-section.
$U_d,\ U_p$	Strain energies of distal and proximal links.
U	Total strain energy of the mechanism.
$\Delta S \in \mathbb{R}^6$	Deflection's vector of the moving platform w.r.t. $\mathbf{s}$.
$\mathbf{tr}_\omega(C)$	Weighted trace of compliance matrix.
ω_i^{adm}	Imposed values of weight factors in $\mathbf{tr}_\omega(C)$.
$\mathrm{T}_{\max}$	Global maximum of $\mathbf{tr}_\omega(C)$.
α_d	Vector of design parameters.
$F_{obj1},\ F_{obj2}$	Objective functions.

1. Introduction and Previous Work

Compared to serial mechanisms, which have an open-ended kinematic architecture, a parallel manipulator is a closed-loop kinematic chain mechanism whose end-effector is linked to the base by several independent kinematic chains.[21,27] For this type of manipulators, there are some potential applications like manufacturing industries where, numerous parallel robot-based machine tool have been designed.[31] The parallel topology offers higher stiffness, lower moving mass, higher accuracy and higher ability to manipulate heavy loads relative to serial kinematic mechanisms. In contrast, these performance are very sensitive to the task uncertainties and to the variation of geometric and structural dimensions of the various links and joints defining the mechanism. Hence, performance indices (or design criteria) are devised to help the designer cope with uncertainty and, to synthesize the best geometric configuration that satisfies practical design requirements.

The main drawback of parallel robots is their small workspace.[25] Therefore, the most obvious consideration in the design process is to maximize the *accessible workspace* that can be reached by the parallel mechanism's end-effector, denoted here by the center of the moving platform. Hence, in this stage we must determine the geometric parameters of the robotic architecture satisfying the workspace requirements. However, when maximum workspace is considered as the only index in designing a parallel robot, it is possible to provide poor kinematic characteristics within some sub-workspaces. In addition, the workspace of a parallel manipulator is bounded by actuated joint limitations, limitations on the passive joint variables and, mechanical interferences between their links. To overcome undesirable effects in workspace, researchers have introduced additional performance measures in the design process. When working on the design of articulated hands, Salisbury and Craig[24] introduced the *kinetostatic* concept of *dexterity*, which is defined as the ability of the mechanism to move and apply forces and torques in arbitrary directions with equal ease.[8,25] Gosselin and Angeles[9,10] analyzed the kinematic design of planar and spherical three degrees of freedom (DoFs) parallel manipulators taking into account the isotropy index. Stock and Miller[26] presented a method for kinematic optimization of the linear DELTA geometric parameters including manipulability as a performance index. For design applications, a global dexterity index is more desirable. Chablat *et al.*[3] presented a comparison study using regular dexterous Cartesian workspace based on the interval analysis method. Lou *et al.*[18] proposed to maximize a regularly shaped workspace under global dexterity constraints. In ref. [17], Liu *et al.* proposed a design method of a DELTA robot based on the concept of maximum inscribed workspace. Liu[16] also presented an optimal kinematic design method of three translational DoFs parallel manipulators, where the related performance criteria are good-conditioning workspace, global conditioning index and global stiffness index. Some other researchers (Lara *et al.*[14] and Li and Xi[15,29]) have considered both performance indices and volume of workspace, simultaneously. Taking the linear DELTA robot as a case of study, Kelaiaia *et al.*[13] presented a design approach based on the combination of several performance measures in a multi-objective optimization process using genetic algorithms. In ref. [22], de-Jean *et al.* presented a multi-criteria

https://doi.org/10.1017/S0263574714001416 Published online by Cambridge University Press

approach for designing DELTA robot with maximum dexterity and minimum projected area of the occupied volume on the base plane. Recently, Zhao[32] considered the velocity transmission index for dimensional synthesis of the DELTA parallel robot. In ref. [28], Johan *et al.* presented a mathematical framework for optimal design of product families and they illustrated the efficiency of multi-objective evolutionary algorithms for industrial robot applications.

In practice, such as milling parallel machine, the highest rigidity and precision are required. Hence, mechanical flexibility of the various links and joints must also be considered in the design process. The study of the mechanism's response to the applied external wrench (force and moment) under static equilibrium belonging to the domain of *elastostatics*.[25] Many researchers have studied the flexibility behavior assuming that elasticity is concentrated in the actuator joint,[8,13] which may be expressed by the *stiffness* of actuated joints. Based on elasto-geometric modeling, Courteille *et al.*[6] proposed a multi-objective formulation with three global stiffness objectives in order to enhancing the rigidity of the DELTA parallel robot but, without considering kinetostatic performance. Assuming that the measure of dexterity is closely related to joint's stiffness,[18] the present paper consider that the flexibility of the parallel manipulator is measured in terms of the deflection of links.

The design process is usually treated as an optimization problem, which refers to finding one or more solutions that correspond to the extreme values of one or more objectives. The design optimization problem deals with multiple conflicting objectives (e.g., workspace and accuracy, link's weight and its deflection). Many researchers treated this problem using a single objective weighted function.[2,30] However, It is difficult to analyze the effect of the weights in the cost function. This approach can only provide a compromise between these antagonistic performance requirements. Formulating the design problem as a multi-objective optimization one can be an ideal alternative. In this case, a set of *non-dominated* solutions, also called *Pareto-optimal* set is obtained. For more details on multi-objective optimization and optimal design application, please refer to refs. [7, 28].

In this paper, we focus on the dimensional-synthesis-based kineto-elastostatic performance optimization of the DELTA parallel mechanism. Accordingly, the main contributions of our paper are:

- We present a design approach to solve the dimensional synthesis problem of the DELTA parallel manipulator. The proposed approach considers simultaneously several performance criteria that have direct impact on the mechanical design of a mechanism. Therefore, we propose to formulate the design problem as a multi-objective optimization one.
- We develop the elastostatic model of the studied DELTA parallel robot using Castigliano's energetic theorem.[23] Meanwhile, the exactitude of the developed model is verified through **ANSYS**® software. Furthermore, we establish the corresponding kineto-elastostatic performance defining the optimization cost functions where, the highest structure's stiffness and the largest dexterous workspace are desired so as to reach high rigidity and precision.
- We implement the proposed approach using **MATLAB**® optimization toolbox and, we present numerical results that show the effectiveness of the proposed design method to enhancing kineto-elastostatic performance of the manipulator's structure.

This paper is organized as follows: Section 2 presents the developed kinematic and elastostatic studies of the DELTA parallel robot. Section 3 introduces the proposed design approach and gives the multi-objective design problem formulation. Section 4 discusses the implementation and the results of the proposed design method. Section 5 concludes the paper.

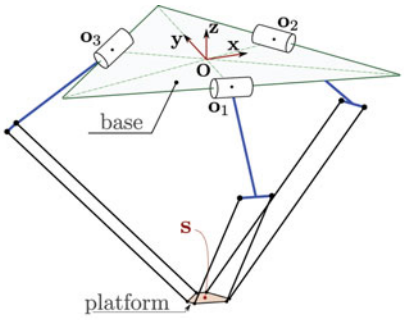
2. Structure Description and Modelling

Without the loss of generality, we use the DELTA robot[4] as an example for our study, this section deals with the development of the kinematic and elastostatic models of its three DoFs structure. Furthermore, these models will be used later to evaluate the corresponding *kineto-elastostatic* performance of the DELTA parallel manipulator.

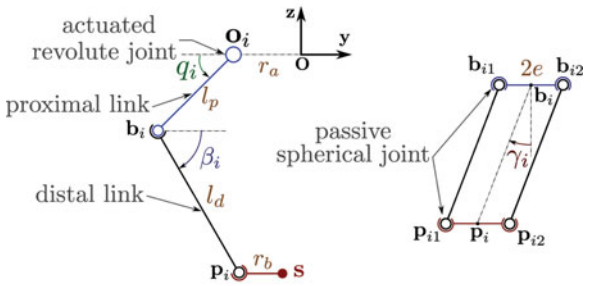
2.1. Geometric representation and kinematics

As shown in Fig. 1(a), the geometric arrangement of the joints and links of the DELTA mechanism provides to the moving platform three translational DoFs. This successful design, proposed by Clavel,[4]

https://doi.org/10.1017/S0263574714001416 Published online by Cambridge University Press



(a) Architecture of the DELTA robot



(b) Geometric description of the $i-$th subchain

Fig. 1. Architecture of the DELTA robot and geometric description of its $i-$th subchain.

is widely used for fast packaging in food industry. The kinematic architecture consists of a base, a moving platform, and three identical subchains.

The fixed reference frame $\mathcal{R}(\mathbf{o}, \mathbf{x}, \mathbf{y}, \mathbf{z})$ supports three actuated *revolute* joints, where their axes form an equilateral triangle in $\mathbf{xy}$-plan, and $\mathbf{oo}_1$ points along the $-\mathbf{y}$-axis. Each subchain contains one spatial *parallelogram* four bar connected by *spherical* joints. The role of the parallelograms is to restrain the orientation of the platform to be parallel to the working surface. The moving platform executes pure spatial translation obtained through the combination of the actuation of the three revolute joints. All geometric parameters are depicted in Fig. 1(b), where l_p denotes the length of the actuated arms $\mathbf{o}_i\mathbf{b}_i$, l_d the length of the parallelogram's bar $\mathbf{b}_{ij}\mathbf{p}_{ij}$ $(i = 1 \dots 3,\ j = 1 \dots 2)$, and $r_a = \| \mathbf{oo}_i \|$, $r_b = \| \mathbf{p}_i\mathbf{s} \|$, where $\mathbf{o}$ and $\mathbf{s}$ are the centers of the base and the platform, respectively. From each subchain, we can derive the loop-closure vector constraint as follows

$$\mathbf{os} = \mathbf{oo}_i + \mathbf{o}_i\mathbf{b}_i + \mathbf{b}_i\mathbf{p}_i + \mathbf{p}_i\mathbf{s} \tag{1}$$

With respect to the fixed reference frame $\mathcal{R}$, the vectorial Eq. (1) gives three scalar equations relating coordinates of the platform center $\mathbf{s} = (x_s,\ y_s,\ z_s)^T$ to angular kinematic variables q_i, β_i and γ_i. By eliminating the passive joint variables β_i and γ_i from (1), we derive the loop-closure equations relating the actuated joint coordinates $\mathbf{q} = (q_1,\ q_2,\ q_3)^T$ to the translation variables $\mathbf{s}$.[5,18]

$$(\lambda_i \sin\psi_i - x_s)^2 + (\lambda_i \cos\psi_i + y_s)^2 + (l_p \sin q_i + z_s)^2 - l_d^2 = 0 \tag{2}$$

for $i = 1 \dots 3$, where $\lambda_i = r + l_p \cos q_i$, $r = r_a - r_b$. $\psi_i = \frac{2\pi}{3}(i-1)$ denotes the angle between the vector $\mathbf{oo}_i$ and $-\mathbf{y}$-axis. Using equations given by (2) we can solve the forward kinematic problem by determining the pose of the platform $\mathbf{s}$ for a given actuated joint coordinates $\mathbf{q}$, or the inverse kinematic problem by expressing the vector $\mathbf{q}$ for a given platform pose $\mathbf{s}$.

2.2. Jacobian matrix and conditioning index

The Jacobian matrix J maps the relationship between the spatial velocity $\dot{\mathbf{s}}$ of the moving platform and the active joint velocities $\dot{\mathbf{q}}$. Differentiation with respect to time of the loop-closure constraints

https://doi.org/10.1017/S0263574714001416 Published online by Cambridge University Press

given in (2) yields a set of equations of the form $J_s\dot{\mathbf{s}} = J_q\dot{\mathbf{q}}$, with

$$J_s = \begin{bmatrix} \mathbf{v}_1 \\ \mathbf{v}_2 \\ \mathbf{v}_3 \end{bmatrix} \; ; \; J_q = \text{diag}(\mathbf{h}) \tag{3}$$

where

$$\mathbf{v}_i = [x_s - \lambda_i \sin\psi_i \;\; y_s + \lambda_i \cos\psi_i \;\; z_s + l_p \sin q_i] \tag{4}$$

and

$$h_i = (y_s \cos\psi_i + r - x_s \sin\psi_i)\, l_p \sin q_i - l_p z_s \cos q_i \tag{5}$$

The function diag($\mathbf{h}$), with $\mathbf{h} = (h_1,\ h_2,\ h_3)^T$ is a vector with 3 components given by (5), returns 3-by-3 diagonal matrix having $\mathbf{h}$ as its main diagonal. Then, the Jacobian matrix of the robot can be written as

$$J(\mathbf{s}, \mathbf{q}) = J_s^{-1} J_q \tag{6}$$

In the design process, the Jacobian matrix is widely used to evaluate kinetostatic performance such as dexterity, manipulability and singularity analysis. A measure of the dexterity can be defined as the *condition number* κ of J. A most general definition of condition number is $\kappa = \| J \| \| J^{-1} \|$, where $\| \cdot \|$ denotes any norm of a matrix. In this paper, the *weighted matrix Frobenius norm* is adopted because it is more significant in engineering and through which the computation of singular values of J can be omitted.[25] For the parallel DELTA robot, the Frobenius condition number κ_F of the kinematic Jacobian is defined as

$$\kappa_F = \frac{1}{3}\sqrt{\mathbf{tr}(J^T J)}\sqrt{\mathbf{tr}(J^T J)^{-1}} \tag{7}$$

with $\mathbf{tr}(\cdot)$ is the sum of the diagonal elements of the matrix.

The *conditioning index* $\mu \in [0, 1]$ is defined as the reciprocal of the Jacobian matrix condition number,[11] which is given by

$$\mu = \frac{1}{\kappa_F} \tag{8}$$

Actually, the conditioning index μ is used to evaluate the dexterity, the isotropy, the distance to the singularity, as well as the static stiffness of a mechanism.[24] Therefore, the larger the conditioning number μ, the well-conditioned the kinematic Jacobian J and the farther the distance to the singularity.[17] Instead of local quality measures, which characterize the dexterity of the mechanism at a given posture (J is configuration dependent), a global measure of the dexterity is more suitable for design applications. For our design approach, we consider the minimum of the conditioning index $\mu_{\min}$, over the required workspace, as the global dexterity measure.

2.3. Regular workspace

Generally, the workspace of a robot is the total volume swept out by the end-effector when the mechanism executes all possible motions. For the parallel DELTA robot, the reachable workspace is restricted by the following limitations[5]

1. The technological limitations on the range of motion of the parallelogram's passive joints. Either universal or spherical joints impose a geometric limitation with same range, so $\gamma^{\max} = 40^\circ$, then

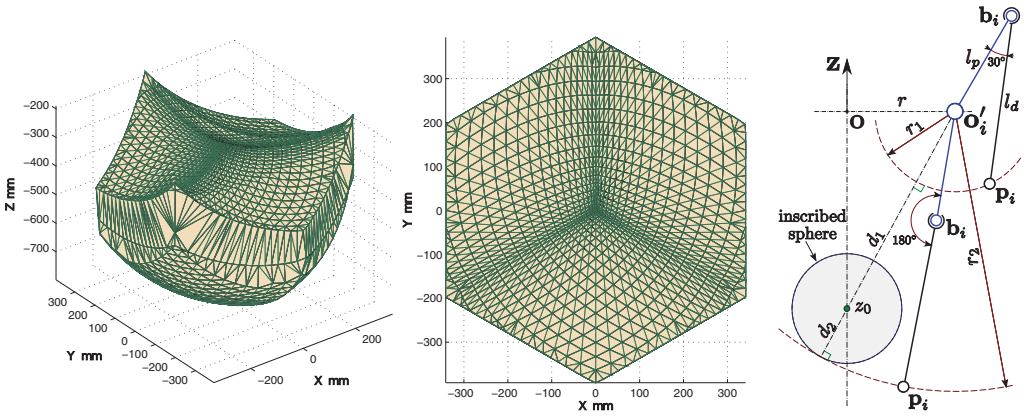
$$-40^\circ \leqslant \gamma_i \leqslant 40^\circ \tag{9}$$

2. The mechanical interferences between the actuated arm and the parallelogram's bars and between the parallel bars and motors when $(q_i + \beta_i)$ is very small. So, this angle must be lower bounded

https://doi.org/10.1017/S0263574714001416 Published online by Cambridge University Press

Table I. Characteristic dimensions of the DELTA−740 robot ($\alpha_1 = 0.631,\ \alpha_2 = 1.846$).

Parameter	l_p	l_d	r_a	r_b
Dimension (mm)	260	480	194	30



(a) Workspace of the DELTA−740. (b) Inscribed sphere

Fig. 2. Geometric representation of the accessible and regular workspaces.

by 30° for the studied mechanism. Also, in order to avoid having multiple solutions of the inverse kinematic problem, the angle $(q_i + \beta_i)$ must be upper bounded by 180°, then

$$30^\circ \leqslant q_i + \beta_i \leqslant 180^\circ \tag{10}$$

In addition of these angular constraints, Clavel[5] has proposed some constraints on the characteristic dimensions of the DELTA robot that allow to avoid singularities. These geometric constraints can be written as follows

$$\alpha_1 = \frac{r}{l_p} \geqslant 0.5\ ;\ \alpha_2 = \frac{l_d}{l_p} \geqslant 1.75 \tag{11}$$

There exist several possible approaches for representing the reachable workspace of parallel robots.[1,12,20] In this paper, and based on the discretization of the configuration space, we generate the 3D plot (defined by triangle mesh) of the workspace. In Fig. 2(a), we depicted the 3D mesh representation of the DELTA−740 robot workspace, whose geometric parameters are summarized in Table I.

For practical cases, a *regular workspace* is generally imposed, which is defined as a sub-workspace where the mechanism can acquire the highest required performance. In this paper, the *maximum inscribed sphere* with radius r_{ball} and centered at point $(0, 0, z_0)$ is considered as the regular workspace (Fig. 2(b)). Considering the constraints (10), the radius r_{ball} of maximum inscribed sphere and the position z_0 are determined analytically as follows

$$r_{ball} = \frac{r_2 - r_1}{2}\ ;\ z_0 = -\sqrt{\left(\frac{r_1 + r_2}{2}\right)^2 - r^2} \tag{12}$$

with $r_1 = \sqrt{l_p^2 + l_d^2 - l_p l_d \sqrt{3}}$ and $r_2 = l_p + l_d$. It should be noted that the maximum inscribed sphere is obtained when $d_1 = d_2$ (refer to Fig. 2(b)).

https://doi.org/10.1017/S0263574714001416 Published online by Cambridge University Press

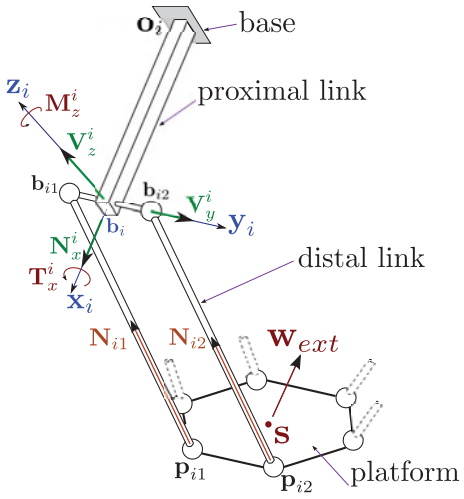


Fig. 3. Internal forces and moments in distal and active proximal links.

According to the above kinetostatic analysis, a set of characteristic parameters can thus be determined as follows

$$\alpha_c = [\alpha_1 \ \alpha_2]^T \tag{13}$$

As expressed in Eq. (11), the dimensionless characteristic parameters α_1 and α_2 of the DELTA robot give the relations between its dimensions. Therefore, if the total size of the mechanism is normalized by the maximum length $l_{\max}$ of a subchain, where $l_p + l_d + r = l_{\max}$, we can compute all geometric dimensions, then

$$l_p = \frac{l_{\max}}{1 + \alpha_1 + \alpha_2} \ ; \ l_d = l_p \alpha_2 \ ; \ r = l_p \alpha_1 \tag{14}$$

2.4. Elastostatic analysis

The above kinetostatic study assumes that the parallel manipulator consist of rigid links. In practice, when the end-effector of the mechanism is subjected to important interacting wrenches, links flexibility must be taken into account when considering robot design. Therefore, we focus on modeling the elastostatic behavior of the DELTA parallel robot, which can be evaluated by the mechanism's response to the external applied wrench $\mathbf{w}_{ext}$ under static equilibrium. In the formulation of the elastostatic model, the moving platform and links $\mathbf{b}_{i1}\mathbf{b}_{i2}$ are treated as rigid bodies.

Under the hypothesis of a linear elastic structure, the *Castigliano*'s theorem can be applied in order to compute the displacements of the DELTA's moving platform, which are given by the partial derivatives of the *total elastic strain energy U* with respect to the external applied loads.[23]

2.4.1. Strain energy of distal links. The distal link is regarded as a homogeneous simple support bar subjected to a normal force $\mathbf{N}_{ij} = N_{ij}\mathbf{u}_i$, with $\mathbf{u}_i = \frac{\mathbf{b}_{i1} - \mathbf{p}_{i1}}{\|\mathbf{b}_{i1} - \mathbf{p}_{i1}\|}$ and $(i = 1, 2, 3, \ j = 1, 2)$. In this paper, the distal link has a solid circular cross-section of diameter ϕ_d. As shown in Fig. 3, point $\mathbf{b}_{ij}$ and $\mathbf{p}_{ij}$ are connected, respectively, with the active proximal link and the moving platform through spherical joints. Hence, the strain energy of the six distal links can be expressed as

$$U_d = \frac{l_d}{2E_d A_d} \sum_{i=1}^{3} (N_{i1}^2 + N_{i2}^2) \tag{15}$$

Where E_d denote the Young's modulus and A_d is the cross sectional area of the distal link. Under static equilibrium with respect to (w.r.t.) the center $\mathbf{s}$ of the moving platform, the six-dimensional

https://doi.org/10.1017/S0263574714001416 Published online by Cambridge University Press

vector $\mathbf{N}_d$ of internal axial forces in the distal links can be related to the external wrench $\mathbf{w}_{ext}$ as

$$\mathbf{N}_d = A\ \mathbf{w}_{ext} \tag{16}$$

where the 6-by-6 matrix A is given as

$$A = \begin{pmatrix} \mathbf{u}_1 & \mathbf{u}_1 & \mathbf{u}_2 & \mathbf{u}_2 & \mathbf{u}_3 & \mathbf{u}_3 \\ \mathbf{v}_{11} & \mathbf{v}_{12} & \mathbf{v}_{21} & \mathbf{v}_{22} & \mathbf{v}_{31} & \mathbf{v}_{32} \end{pmatrix}^{-1}$$

and

$$\mathbf{u}_i = \tfrac{\mathbf{b}_{i1}-\mathbf{p}_{i1}}{\|\mathbf{b}_{i1}-\mathbf{p}_{i1}\|}\ ;\ \mathbf{v}_{ij} = (\mathbf{p}_{ij} - \mathbf{s}) \times \mathbf{u}_i$$
$$\mathbf{N}_d = (N_{11}\ N_{12}\ N_{21}\ N_{22}\ N_{31}\ N_{32})^T\ ;\ \mathbf{w}_{ext} = \left(f_x\ f_y\ f_z\ \tau_x\ \tau_y\ \tau_z\right)^T$$

2.4.2. Strain energy of active proximal links. The active proximal link is considered as a homogeneous cantilever beam. In this paper, the proximal link has a solid rectangular cross-section of dimensions $b \times h$. As shown in Fig. 3, this link is subjected to axial, bending, shear, and torsional forces. Hence, the strain energy of proximal links is given by

$$U_p = \frac{l_p}{2}\sum_{i=1}^{3}\left[\frac{(N_x^i)^2}{E_pA_p} + \frac{k_y(V_y^i)^2}{G_pA_p} + \frac{l_p^2(V_y^i)^2}{3E_pI_{zp}} + \frac{k_z(V_z^i)^2}{G_pA_p} + \frac{l_p^2(V_z^i)^2}{3E_pI_yp} + \frac{(T_x^i)^2}{G_pJ_p} + \frac{(M_z^i)^2}{E_pI_{zp}} + \frac{l_pV_y^iM_z^i}{E_pI_{zp}}\right] \tag{17}$$

where E_p is Young's modulus, G_p is the shear modulus, A_p is the cross sectional area of the proximal link, I_{yp}, I_{zp} are the bending moments of inertia, k_y, k_z are the shear section constants and J_p is the torsional moment of inertia. By applying the balance on point $\mathbf{b}_i$ and w.r.t. the proximal link coordinate system $(\mathbf{b}_i, \mathbf{x}_i, \mathbf{y}_i, \mathbf{z}_i)$, the internal forces and moments in Eq. (17) can be related to the distal links internal forces N_{ij} as follows:

$$\mathbf{F}_p^i = \begin{pmatrix} N_x^i \\ V_y^i \\ V_z^i \\ T_x^i \\ M_z^i \end{pmatrix} = \begin{pmatrix} \epsilon_i & \epsilon_i \\ \xi_i & \xi_i \\ \chi_i & \chi_i \\ -\sigma_i & \sigma_i \\ -\gamma_i & \gamma_i \end{pmatrix} \begin{pmatrix} N_{i1} \\ N_{i2} \end{pmatrix} \tag{18}$$

where

$$\begin{aligned} \epsilon_i &= \mathbf{u}_i \cdot \mathbf{x}_i \\ \xi_i &= \mathbf{u}_i \cdot \mathbf{y}_i \\ \chi_i &= \mathbf{u}_i \cdot \mathbf{z}_i \\ \sigma_i &= e(\mathbf{y}_i \times \mathbf{u}_i) \cdot \mathbf{x}_i \\ \gamma_i &= e(\mathbf{y}_i \times \mathbf{u}_i) \cdot \mathbf{z}_i \end{aligned}$$

2.4.3. Total strain energy and deflections. Given an external generalized force $\mathbf{w}_{ext}$ applied to the center $\mathbf{s}$ of the moving platform and using Eqs. (15) and (17), the total strain energy due to the external generalized force can be expressed as

$$U = U_d + U_p \tag{19}$$

https://doi.org/10.1017/S0263574714001416 Published online by Cambridge University Press

The strain energy U_p in Eq. (17) can be expressed as a function of internal forces N_{ij} using Eq. (18). So, the total elastic strain energy of the DELTA robot is given by

$$U = \sum_{i=1}^{3} \left[\frac{1}{2} \left(\bar{\rho}_{i1} N_{i1}^2 + \bar{\rho}_{i2} N_{i2}^2 \right) + \bar{\mu}_i N_{i1} N_{i2} \right] \tag{20}$$

where

$$\bar{\rho}_{i1} = \rho_i - l_p^2 \frac{\xi_i \gamma_i}{E_p I_{zp}} \; ; \; \bar{\rho}_{i2} = \rho_i + l_p^2 \frac{\xi_i \gamma_i}{E_p I_{zp}}$$
$$\bar{\mu}_i = l_p \left[\frac{\epsilon_i^2}{E_p A_p} + \frac{k_y \xi_i^2}{G_p A_p} + \frac{l_p^2 \xi_i^2}{3 E_p I_{zp}} + \frac{k_z \chi_i^2}{G_p A_p} + \frac{l_p^2 \chi_i^2}{3 E_p I_{yp}} - \frac{\sigma_i^2}{G_p J_p} - \frac{\gamma_i^2}{E_p I_{zp}} \right]$$

and

$$\rho_i = l_p \left[\frac{\epsilon_i^2}{E_p A_p} + \frac{k_y \xi_i^2}{G_p A_p} + \frac{l_p^2 \xi_i^2}{3 E_p I_{zp}} + \frac{k_z \chi_i^2}{G_p A_p} + \frac{l_p^2 \chi_i^2}{3 E_p I_{yp}} + \frac{\sigma_i^2}{G_p J_p} + \frac{\gamma_i^2}{E_p I_{zp}} \right] + \frac{l_d}{E_d A_d}$$

Therefore, the total strain energy can be evaluated for a given configuration of the DELTA mechanism by using Eq. (20). The internal forces N_{ij} are computed from (16) for a given applied external wrench $\mathbf{w}_{ext}$.

In order to compute the displacement vector $\Delta S = (\delta_x \; \delta_y \; \delta_z \; \theta_x \; \theta_y \; \theta_z)^T$ of the center $\mathbf{s}$ of the moving platform w.r.t. the fixed reference frame $\mathcal{R}(\mathbf{o}, \mathbf{x}, \mathbf{y}, \mathbf{z})$, we use the Castigliano's theorem for displacements in a linearly elastic structure. So, the partial derivative of the strain energy w.r.t. generalized force gives the generalized displacement in the direction and location of the displacement. Hence, the vector ΔS can be expressed as follows

$$\Delta S = A^T B A \, \mathbf{w}_{ext} = C \, \mathbf{w}_{ext} \tag{21}$$

where the 6-by-6 matrix $C = A^T B A$ denotes the compliance matrix of the mechanism and B is a 6-by-6 matrix given as

$$B = \begin{pmatrix} B_1 & \mathbf{0}_2 & \mathbf{0}_2 \\ \mathbf{0}_2 & B_2 & \mathbf{0}_2 \\ \mathbf{0}_2 & \mathbf{0}_2 & B_3 \end{pmatrix} \text{ with } B_i = \begin{pmatrix} \bar{\rho}_{i1} & \bar{\mu}_i \\ \bar{\mu}_i & \bar{\rho}_{i2} \end{pmatrix} \tag{22}$$

Stiffness is a very important factor in many applications. For example, the induced vibration is explicitly related to the stiffness of machine tool. In this case, high stiffness allows greater machining speeds and feeds while providing the desired precision which reduces chatter.[31] Using the compliance matrix C, the distribution of the structure's compliance over the workspace is the distribution of the trace of C because the trace is an invariant of the matrix. Hence, we introduce the following weighted trace of the compliance matrix

$$\mathbf{tr}_\omega(C) = \sum_{i=1}^{6} \omega_i \, c_{ii} \tag{23}$$

where, c_{ii} denotes the diagonal elements of the structure's compliance matrix and, ω_i is weight factor for each directional compliance which is used in optimization process to define constraints. These weight factors are used by the designer to facilitate maximizing the structural rigidity along certain directions over others. Therefore, the choice of these coefficients is related to the compliance distribution all over the regular workspace as well as the task to be performed.

https://doi.org/10.1017/S0263574714001416 Published online by Cambridge University Press

Table II. Static parameters of the DELTA−740 structure.

E_d (GPa)	E_p (GPa)	G_p (GPa)	A_d mm^2	A_p mm^2	I_{yp} mm^4	I_{zp} mm^4	J_p mm^4
220	72	26.9	28.3	378	13892	10206	20161

Table III. Comparisons between analytical model and ANSYS model.

$\mathbf{q} = (q_1\ q_2\ q_3)^T\ (degrees)$		(10 10 10)	(15 45 75)	(30 10 5)
ANSYS model	$\delta_s\ (\mu m)$	245	407.5	266.5
	$\theta_s\ (10^{-6} rad)$	13178.1	10165.2	12439
Analytical model	$\delta_s\ (\mu m)$	244.8	407.4	266.5
	$\theta_s\ (10^{-6} rad)$	13178.9	10165.1	12438.5

2.4.4. Validation of the elastostatic model. The six components of deflection vector ΔS can be regrouped into two scalars. The first scalar δ_s denotes the displacement vector sum and, the second scalar θ_s denotes the rotation angle. They are expressed as follows

$$\delta_s = \left(\delta_x^2 + \delta_y^2 + \delta_z^2\right)^{\frac{1}{2}}\ ;\ \theta_s = \mid \arccos \varepsilon_0 \mid \tag{24}$$

where the unit quaternions $(\varepsilon_0\ \varepsilon_2\ \varepsilon_2\ \varepsilon_3)^T$ are used to describe the orientation defined by the three angles $(\theta_x\ \theta_y\ \theta_z)$. Note that unit quaternions are closely related to the angle-axis representation of orientation, where ε_0 corresponds to the angle of rotation, while ε_1, ε_2, and ε_3 define the axis of rotation.[25]

In order to verify the exactitude of the developed elastostatic model, we have developed a model of the DELTA mechanism under the ANSYS-apdl finite element code. The results obtained using the programmed model in software ANSYS are compared to those obtained using the analytical elastostatic model. As an example, the prototype DELTA−740 is subjected to an external wrench $\mathbf{w}_{ext} = (10N\ \ -7N\ 12N\ 9Nm\ 5Nm\ \ -3Nm)^T$ w.r.t. the center $\mathbf{s}$ of the moving platform. The dimensional and inertia parameters of the structure are shown in Tables I and II. In this example, the proximal link has a solid rectangular cross-section of dimension 21×18 (mm^2) where the shear correction constants are $k_y = k_z \simeq 1.2$. The distal link has a solid circular cross-section of diameter 6 mm. For different joint configurations $\mathbf{q}_i = (q_{i1}\ q_{i2}\ q_{i3})^T$ of the mechanism, Table III gives a comparison between the results obtained from ANSYS and those computed by the developed elastostatic model using equation (20).

The coherent results of Table III, show the efficiency of the analytical model to measure the elastostatic performance of the DELTA structure. It should be noted that under ANSYS, the model evaluation requires an average runtime of 2 seconds. However, the analytical model needs only 5 ms under MATLAB, which is a significantly less computational runtime than the one needed by a finite element code. Therefore, compared to traditional CAD-FEA approach, this analytical modeling gives a realistic stiffness description as well as a reduction of computational time which allow its use in a parametric optimization loop.

According to the above elastostatic analysis, a set of characteristic parameters can thus be determined as follows

$$\alpha_s = [b\ h\ \phi_d\ e\ r_s]^T \tag{25}$$

where $b \times h$ is the solid rectangular cross-section of the proximal links, ϕ_d is the diameter of the solid circular cross-section of the distal links, the distance $2e$ is between the parallel bars of parallelograms (refer to Fig. 1) and, $r_s \in [0, r_{ball}]$ is the radius of the regular spherical workspace.

Therefore, we denote α_d the vector of parameters that describe the geometric and structural dimensions of the parallel manipulator DELTA. According to relations (13) and (25), we define the

https://doi.org/10.1017/S0263574714001416 Published online by Cambridge University Press

components of this vector as follow:

$$\alpha_d = [\alpha_1\ \alpha_2\ b\ h\ \phi_d\ e\ r_s]^T \tag{26}$$

3. Design Optimization

The detailed analysis of the kinematics and elastostatics of the DELTA parallel mechanism conducted in previous sections will now be used to define and optimize its geometric and structural parameters. The purpose of optimization design is to enhance the performance criteria by adjusting these parameters. Therefore, the main problematic is how to find the best design parameter vector α_d such that the variation of the specified kineto-elastostatic performance is minimum over the regular workspace.

3.1. Problem statement

The design optimization problem can be stated as follows: let α_d denote the vector of parameters that describe the geometric and structural dimensions of the parallel manipulator and, try to find the optimal solution α_d^*. This solution corresponds to the optimal mechanical structure according to given performance criteria while all constraints are respected.

3.2. Constraints

Generating feasible solutions is restricted by numerous constraints that must be satisfied. These constraints concern boundary conditions and the specified kineto-elastostatic performance.

• **Boundary conditions**: They define a search domain for each optimization variable. Hence, the vector of the geometric and static dimensions, which is defined in (26), must satisfy the following constraints:

$$\alpha_d^{\min} \leqslant \alpha_d \leqslant \alpha_d^{\max} \tag{27}$$

where

$$\begin{aligned} \alpha_d^{\min} &= [\ 0.5 \quad 1.75 \quad b^{\min} \quad h^{\min} \quad \phi_d^{\min} \quad e^{\min} \quad 0\ ]^T \\ \alpha_d^{\max} &= [\ \alpha_1^{\max} \quad \alpha_2^{\max} \quad b^{\max} \quad h^{\max} \quad \phi_d^{\max} \quad e^{\max} \quad r_{ball}\ ]^T \end{aligned} \tag{28}$$

It should be noted that the knowledge of all technological considerations and task requirements can help designer to define lower boundary conditions. The upper boundary conditions can be set coarsely where the optimization process will attempt to compute trade-offs between the rigidity of the structure and its mass. Additional conditions that are implicitly considered specify the maximum dimension $l_{\max}$ of the manipulator's subchain, the angular constraints defined in relations (9) and (10), and non-singularity constraints defined in (11).

• **Specified performance**: For the manipulator studied here, the highest global stiffness are desired which can be achieved through minimizing the global compliances. The manipulator's pure compliance in each Cartesian direction is defined by the corresponding diagonal element of the matrix C. Hence, to guarantee the minimum variation of elastostatic performance over the regular workspace, we impose the following constraints

$$\text{for } i = 1 \ldots 6 \quad \omega_i = \omega_i^{\text{adm}} \tag{29}$$

These equality constraints characterize the property of the compliance along each Cartesian direction. As mentioned before, the admissible weight factors ω_i^{adm} are fixed by the designer.

In order to guarantee that the regular workspace is effective, a constraint on the conditioning index μ is introduced to characterize the quality of the regular workspace. Hence, we impose the following constraint

$$\mu_{min} \geqslant \mu^{\text{adm}} \tag{30}$$

where, μ_{min} is the global dexterity measure which is the minimum of the conditioning index over the regular workspace. The admissible conditioning index μ^{adm} is imposed by the designer. It should

https://doi.org/10.1017/S0263574714001416 Published online by Cambridge University Press

be noted that a reciprocal of the Frobenius condition number of $\mu^{\text{adm}} \geqslant 0.3$ corresponds to a good dexterity distribution.[18]

3.3. Objective functions

Before formulating the main optimization design problem, we introduce two optimization procedures in order to find end-effector's locations that correspond to poor kineto-elastostatic performance. So, the first procedure computes the mechanism's configuration in which the value of conditioning index μ is minimal and, the second one evaluates the location of the moving platform in which the weighted trace $\mathbf{tr}_{\omega}(C)$ has a maximum value denoted $\mathrm{T}_{\max}$. Since kinematic and elastostatic performance are considered simultaneously, the design problem is formulated as a multi-objective optimization problem. The basic concept of multi-objective optimization is the concept of domination.[31] Therefore, we obtain a set of *non-dominated* solutions, which is also called the *Pareto-optimal* set.[7] The Pareto-optimal set yields an infinite set of solutions on the boundary of the feasible region, from which the desired solution can be chosen.

Many criteria can be chosen as performance index for the proposed optimization problem. The proposed two objective functions are established based on the kinematics and elastostatics studies detailed previously. In this work, objective functions are expressed as follows

$$\begin{aligned} F_{obj1} &= -\min\left[r_{ball}\frac{\mu_{\min}}{\mu^{\text{adm}}},\ r_{ball}\right] \\ F_{obj2} &= m_0 \mathrm{T}_{\max} \end{aligned} \tag{31}$$

where, m_0 denotes the mass of moving bodies in one subchain (proximal links and parallelogram), function min returns the smallest scalar.

The first objective function F_{obj1} is related to the kinematic performance where the problem is to find the optimal geometric parameters that maximize globally the dexterous regular workspace. However, if the minimum dexterity $\mu_{\min}$ is less than the admissible value μ^{adm}, the regular workspace radius r_{ball} will be reduced by multiplying it by the ratio of dexterities. Simultaneously, the second objective function F_{obj2} is introduced to increase elastostatic performance of the robot trying to find the optimum geometric and structural parameters that maximize globally the stiffness of the structure while minimizing its mass. Therefore, the proposed multi-objective optimization problem can be formally represented as follows:

$$\min\left\{F_{obj1}, F_{obj2}\right\} \text{ subject to } \begin{array}{l} l_p + l_d + r = l_{\max} \\ \alpha_d^{\min} \leqslant \alpha_d \leqslant \alpha_d^{\max} \\ \omega_i = \omega_i^{\text{adm}}\ i = 1 \ldots 6 \\ \mu_{min}\left(J(\mathbf{s}, \mathbf{q})\right) \geqslant \mu^{\text{adm}} \end{array} \tag{32}$$

As described in the beginning of this subsection, the values of the minimum dexterity $\mu_{\min}$ and the maximum compliance $T_{\max}$ are computed before each evaluation of functions F_{obj1} and F_{obj2}. The values of weight factors ω_i^{adm} are mainly dependent on the desired precision degree along each Cartesian direction.

3.4. Resolution techniques

In the case of multi-objective optimization problems, it is not necessary to have the best solution due to conflicts among objective functions when an improvement in one objective requires a degradation of another. Therefore, the result is a set of non-dominated or Pareto-optimal solutions. To find the optimal Pareto front, we use the Controlled Elitist Non-dominated Sorting Genetic Algorithm (CENSGA) which is a variant of NSGA-II.[7] CENSGA offers a quantitative control of the elite members of the population as the algorithm progresses, which favors individuals that can help increase the diversity of the population even if they have a lower fitness value.[7] Furthermore, the Simulated Annealing technique (SA) is used to explore globally the regular workspace in order to find the values of the minimum dexterity $\mu_{\min}$ and the maximum compliance $T_{\max}$. These quantities are used by CENSGA in each evaluation of the cost functions F_{obj1} and F_{obj2}.

https://doi.org/10.1017/S0263574714001416 Published online by Cambridge University Press

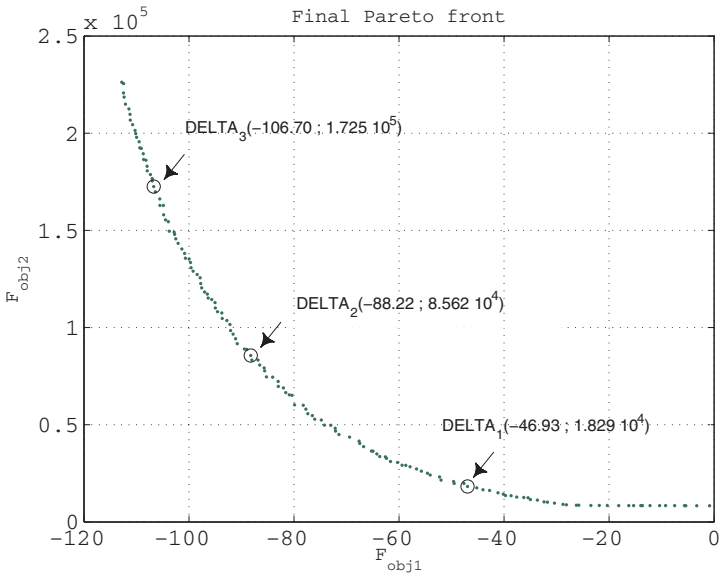


Fig. 4. Pareto-optimal frontier sets in criterion space with three selected solutions.

4. Implementation and Results

The implementation is performed using MATLAB optimization tool.[19] In this research work, the inertial parameters of the various links are defined in Table II and, the mechanism size is normalized by subchain normalization $l_{\max} = 1\ m$. The lower bound of dexterity is given as $\mu^{\text{adm}} = 0.3$. In order to guarantee the minimum variation of elastostatic performance over the regular workspace, we impose the constraints $\omega_i^{\text{adm}} = 10^8$ for each directional compliance. To satisfy some technological constraints such as tool dimensions for example, we can impose that $r_b = 50\ mm$. For the search domain, the optimization variables must satisfy the following boundary conditions:

$$\alpha_d^{\min} = [0.5\ 1.75\ 10\ 10\ 10\ 10\ 0]^T \quad \alpha_d^{\max} = [10\ 10\ 100\ 100\ 50\ 200\ r_{ball}]^T$$

where, the radius r_{ball} of the maximum inscribed sphere is computed at each evaluation of cost functions using relation (12).

Figure 4 shows the Pareto-optimal frontier sets which represent all possible and optimal solutions in decision space. Hence, the designer can intuitively select the final solutions according to its preferences, which reduce the time of design process. From the 150 different solutions obtained in multi-objective optimization, we have selected three robots DELTA$_i$ ($i = 1,\ 2,\ 3$) from the Pareto-optimal solutions (refer to Fig. 4). The corresponding CAD models of the selected solutions are depicted in Fig. 5. For each selected solution, Table IV gives the corresponding set of optimal design parameters.

The robot DELTA$_3$ is chosen as an example, its design parameters are depicted in the last column of Table IV. In Fig. 6, we present the distribution of the dexterity μ, the displacement δ_s and the rotation θ_s of the moving platform when it sweeps the **xy**-plan at $z = z_0$. These distributions are computed when the parallel manipulator DELTA$_3$ is subjected to an external wrench $\mathbf{w}_{ext} = (50N\ 50N\ 100N\ 10Nm\ 10Nm\ 20Nm)^T$ w.r.t. the center of its moving platform.

In Fig. 6(b), we present the distribution of dexterity when the matrix 2-norm is adopted as used in the majority of related works.[18] Hence, for the manipulator DELTA$_3$, the minimum value of the inverse condition number is 0.710 and the maximum value is 0.931, which give a very good dexterity distribution all over the regular workspace.[17] Comparing with results obtained by Lou *et al.*,[18] where the variation interval of inverse conditioning number is [0.4, 0.65], we can easily conclude a net improvement of kinematic performance of the proposed solution. Figure 6(a) shows distribution of inverse condition number when the weighted matrix Frobenius norm is adopted, the minimal value of μ in the regular workspace is 0.32 which is very close to the prescribed threshold $\mu^{\text{adm}} = 0.3$.

https://doi.org/10.1017/S0263574714001416 Published online by Cambridge University Press

Table IV. Geometric and structural dimensions of the selected solutions.

Dimension	DELTA$_1$	DELTA$_2$	DELTA$_3$
α_1	4.49	1.74	1.14
α_2	6.01	2.79	2.14
$b\ (mm)$	24.02	20.61	20.79
$h\ (mm)$	18.75	19.86	20.97
$\phi_d\ (mm)$	10.02	10.03	10.04
$e\ (mm)$	41.49	36.13	35.14
$r_s\ (mm)$	65.11	129.12	162.10
$m_0\ (kg)$	2.27	2.49	2.70
$r_{ball}\ (mm)$	80.06	162.89	206.93
$l_p\ (mm)$	86.94	180.78	233.66
$l_d\ (mm)$	522.22	503.78	499.44
$r\ (mm)$	390.84	315.43	266.90
$z_0\ (mm)$	−356.64	−415.51	−453.44

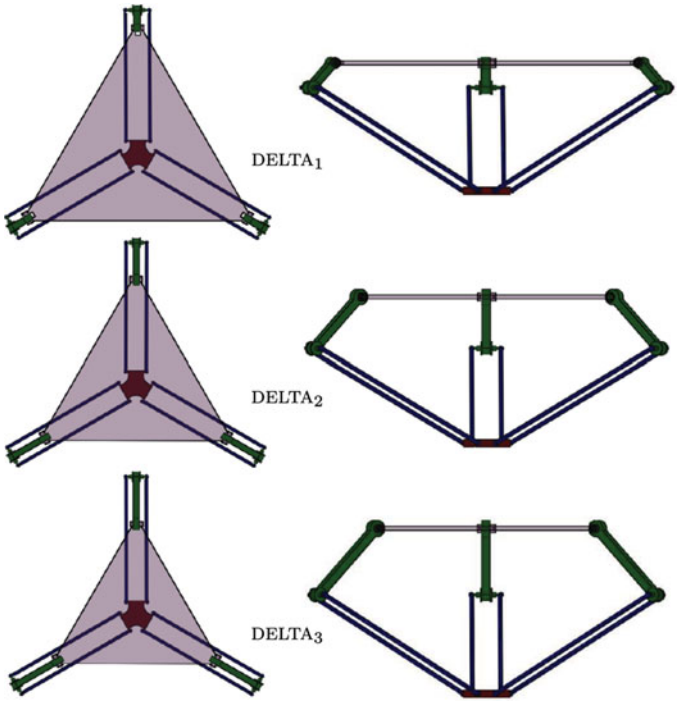
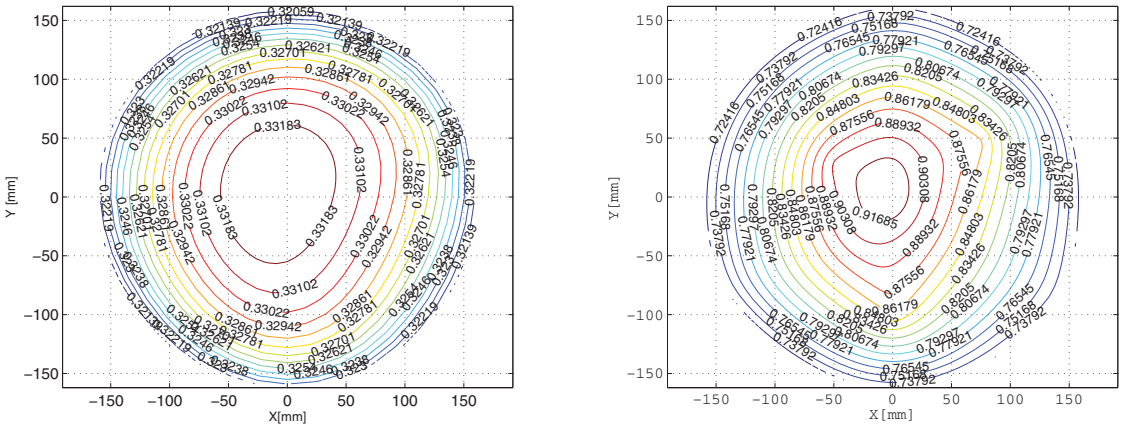


Fig. 5. CAD models of the selected solutions.

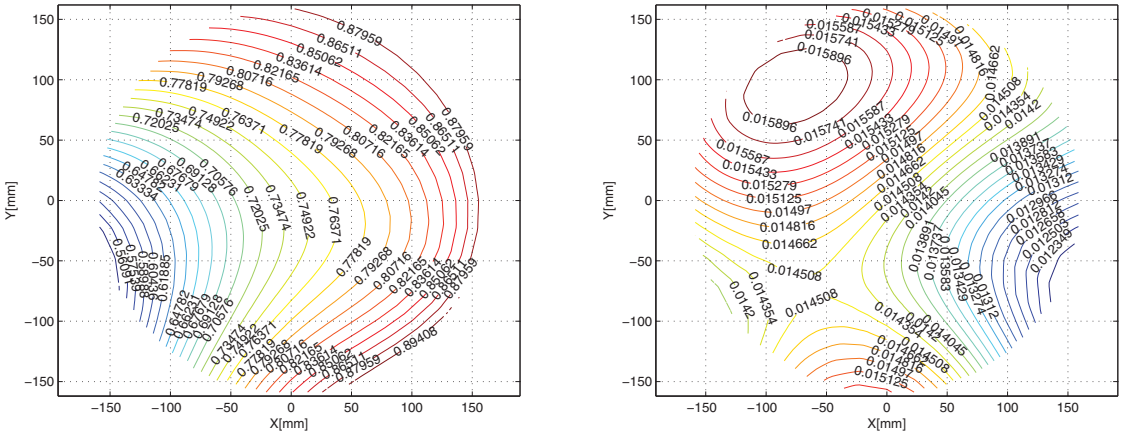
For elastostatic performance of the robot DELTA$_3$, Figs. 7(a) and 7(b) show respectively, distribution of the displacement and rotation of the moving platform in the plane $z = z_0$. We can easily observe the low variation of the manipulator's deformation all over the regular workspace, where the variation intervals are: $\delta_s \in [0.529, 0.910] mm$ and $\theta_s \in [12, 16]\, mrad$. Therefore, despite the higher applied external wrench $\mathbf{w}_{ext}$, the synthesized parallel manipulator has improved elastostatic characteristics compared with its low optimized mass $m_0 = 2.7kg$. In order to show the stiffness improvement, we give a comparison between manipulators DELTA$_3$ and the design ID2556 of [6]. The mass of $ID2556$ robot is $20.2Kg$ and, for a payload of $-800N$ applied along $\mathbf{z}$ axis on the $ID2556$, the maximal displacement of the moving platform is $3.65\, mm$ and the mean value is $1.26\, mm$.[6] Applying the same external wrench on the DELTA$_3$ robot, the maximal obtained displacement is $4.1\ mm$ with a mean value of $3.75\, mm$. Hence, despite the reduced mass of the DELTA$_3$ w.r.t. $ID2556$ solution, the elastostatic performance remain excellent and uniform, even higher payload are applied. It should be noted that the developed elastostatic model can be used to improve robot's accuracy through elastogeometric calibration in order to compensate for the mechanism's deformation.

https://doi.org/10.1017/S0263574714001416 Published online by Cambridge University Press



(a) Dexterity using Frobenius norm (b) Dexterity using 2-norm

Fig. 6. Distributions of dexterity measures of DELTA$_3$ at $z_0 = -453.44\ mm$.



(a) Displacement in mm (b) Rotation in rad

Fig. 7. Distributions of elastostatic performance of DELTA$_3$ at $z_0 = -453.44\ mm$.

5. Conclusion

An optimization method for enhancing kineto-elastostatic performance of the DELTA parallel manipulator is presented in this work. Based on performed kinematic and elastostatic studies, optimal criteria were expressed in order to synthesize a DELTA parallel manipulator with improved performance such as uniformity of the dexterity, largest regular workspace, highest global stiffness, and reduced moving mass. Due to the conflicts among previous objective functions, we proposed to formulate the design problem as a multi-objective optimization one. The CENSGA was proved to be an efficient and reliable optimization tool. Optimal design based kineto-elastostatic performance for the DELTA robot was carried out and the results show the effectiveness of the proposed design procedure. It should be noted that the proposed design approach is original in the sense that it is systematic and it can be applied to any serial and parallel mechanisms for which stiffness and dexterity are critical issues. Pareto-optimization may be considered as a tool providing all possible trade-offs among multiple cost functions that conflict with each other, under different constraints. The final choice remains always subjective and is left to the designer responsibility.

In our future work, elastodynamic performance would be considered during design process in order to avoid a specific spectrum of excitation frequencies under the most likely operation conditions. Also, integrating a Response Surface Methodology to reduce the computation time of the global optimization process could be an interesting extension of our work.

https://doi.org/10.1017/S0263574714001416 Published online by Cambridge University Press

Acknowledgment
I would like to thank the editors and unnamed reviewers for their valuable comments. I would also like to gratefully acknowledge Dr. M. HADDAD for the helpful discussions.

References

1. F. A. Adkins and E. J. Haug, "Operational envelope of a spatial stewart platform," *Trans. ASME, J. Mech. Des.* **2**(119), 330–332 (1997).
2. S. Bhattacharya, H. Hatwal and A. Ghosh, "On the optimum design of a stewart platform type parallel manipulators," *Robotica* **13**(2), 133–140 (1995).
3. D. Chablat, P. Wenger, F. Majou and J-P. Merlet, "An interval analysis based study for the design and the comparison of three-degrees-of-freedom parallel kinematic machines," *Int. J. Robot. Res.* **23**(6), 615–624 (2004).
4. R. Clavel, "Delta, a Fast Robot with Parallel Geometry," *Proceedings of the 18th International Symposium on Industrial Robots, Lausanne* (1988) pp. 91–100.
5. R. Clavel, Conception d'un robot parallèle rapide à quatre degrés de liberté. PhD thesis (EPFL, Lausanne, 1991).
6. E. Courteille, D. Deblaise and P. Maurine, "Design optimization of a delta-like parallel robot through global stiffness performance evaluation," (Oct. 2009) pp. 5159–5166.
7. K. Deb, *Multi-Objective Optimization using Evolutionary Algorithms* (John Wiley & Sons, 2001).
8. C. Gosselin, "Stiffness mapping for parallel manipulators," *IEEE Trans. Robot. Autom.* **3**(6), 377–382 (1990).
9. C. Gosselin and J. Angeles, "The optimum kinematic design of a planar three-degree-of-freedom parallel manipulator," *ASME J. Mech. Des.* **110**(1), 35–41 (1988).
10. C. Gosselin and J. Angeles, "The optimum kinematic design of a spherical three-degree-of-freedom parallel manipulator," *ASME J. Mech. Des.* **111**(2), 202–207 (1989).
11. C. Gosselin and J. Angeles, "A global performance index for the kinematic optimization of robotic manipulators," *Trans. ASME J. Mech. Des.* (113), 220–226 (1991).
12. E. J. Haugh, F. A. Adkins, and C. M. Luh, "Operational envelopes for working bodies of mechanisms and manipulators," *Trans. ASME J. Mech. Des.* **1**(120), 84–91 (1998).
13. R. Kelaiaia, O. Companya and A. Zaatri, "Multiobjective optimization of parallel kinematic mechanisms by the genetic algorithms," *Robotica* **30**(5), 783–797 (2012).
14. F. A. Lara-Molina, J. M Rosrio and D. Dumur, "Multi-objective design of parallel manipulator using global indices," *Open Mech. Eng. J.* **4**, 37–47 (2010).
15. Y. Li and Q. Xu, "A new approach to the architecture optimization of a general 3-puu translational parallel manipulator," *J. Int. Robot. Syst.* **46**(1), 59–72 (2006).
16. X.-J. Liu, "Optimal kinematic design of a three translational dofs parallel manipulator," *Robotica* **24**(2), 239–250 (2006).
17. X.-J. Liu, J. Wang, K.-K. Oh and J. Kim, "A new approach to the design of a delta robot with a desired workspace," *J. Intell. Robot. Syst.* **39**(2), 209–225 (2004).
18. Y. Lou, G. Liu and Z. Li, "Randomized optimal design of parallel manipulators," *IEEE Trans. Autom. Sci. Eng.* **5**(2), 223–233 (2008).
19. MathWorks. *Global Optimization Toolbox, Multiobjective Optimization, UsersGuide* (2012).
20. J.-P. Merlet, "Determination of 6d workspaces of gough-type parallel manipulator and comparison between different geometries," *Int. J. Robot. Res.* **9**(18), 902–916 (1999).
21. J. P. Merlet. *Parallel Robots*, 2nd edn. (Springer Publishing Company, Incorporated, 2010) pp. 12–62.
22. D. Pisla, M. Ceccarelli, M. Husty and B. Corves, *New Trends in Mechanism Science: Analysis and Design* (Springer Dordrecht Heidelberg, London, New York, 2010) pp. 633–640.
23. J. S. Przemieniecki," *Theory of Matrix Structural Analysis* (Courier Dover Publications, 1985).
24. J. K. Salisbury and J. J. Craig, "Articulated hands: force control and kinematic issues," *Int. J. Robot. Res.* **1**(1), 4–17 (1982).
25. B. Siciliano and O. Khatib, *Handbook of Robotics* (Springer, 2008) pp. 229–319.
26. M. Stock and K. Miller, "Optimal kinematic design of spatial parallel manipulators: application to linear delta robot," *ASME J. Mech. Des.* (125), 292–301 (2003).
27. L. W. Tsai, *Robot Analysis, the Mechanics of Serial and Parallel Manipulators* (John Wiley & Sons, 1999).
28. L. Wang, Amos H. C. Ng and K. Deb, *Multi-objective Evolutionary Optimisation for Product Design and Manufacturing* (Springer, 2011).
29. Q. Xu and Y. Li, "Kinematic analysis and optimization of a new compliant parallel micromanipulator," *Int. J. Adv. Robot. Syst.* **3**(4), 59–72 (2006).
30. K. E. Zanganeh and J. Angeles, "Kinematic isotropy and the optimum design of parallel manipulators," *Int. J. Robot. Res.* **16**(2), 185–197 (1997).
31. D. Zhang. *Parallel Robotic Machine Tools* (Springer, 2010).
32. Y. Zhao, "Dimensional synthesis of a three translational degrees of freedom parallel robot while considering kinematic anisotropic property," *Robot. Comput.-Integr. Manuf.* **29**(1), 169–179 (2013).

https://doi.org/10.1017/S0263574714001416 Published online by Cambridge University Press